Journal of Polymers and the Environment (2019) 27:84–96
https://doi.org/10.1007/s10924-018-1324-2

ORIGINAL PAPER

In Situ Compatibilization of Biopolymer Ternary Blends by Reactive Extrusion with Low-Functionality Epoxy-Based Styrene–Acrylic Oligomer

L. Quiles-Carrillo[1] · N. Montanes[1] · J. M. Lagaron[2] · R. Balart[1] · S. Torres-Giner[1,2]

Published online: 26 October 2018

Abstract
The present study reports on the use of low-functionality epoxy-based styrene–acrylic oligomer (ESAO) to compatibilize immiscible ternary blends made of poly(3-hydroxybutyrate-*co*-3-hydroxyvalerate) (PHBV), polylactide (PLA), and poly(butylene adipate-*co*-terephthalate) (PBAT). The addition during melt processing of low-functionality ESAO at two parts per hundred resin (phr) of biopolymer successfully changed the soften inclusion phase in the blend system to a thinner morphology, yielding biopolymer ternary blends with higher mechanical ductility and also improved oxygen barrier performance. The compatibilization achieved was ascribed to the in situ formation of a newly block terpolymer, i.e. PHBV-*b*-PLA-*b*-PBAT, which was produced at the blend interface by the reaction of the multiple epoxy groups present in ESAO with the functional terminal groups of the biopolymers. This chemical reaction was mainly linear due to the inherently low functionality of ESAO and the more favorable reactivity of the epoxy groups with the carboxyl groups of the biopolymers, which avoided the formation of highly branched and/or cross-linked structures and thus facilitated the films processability. Therefore, the reactive blending of biopolymers at different mixing ratios with low-functionality ESAO represents a straightforward methodology to prepare sustainable plastics at industrial scale with different physical properties that can be of interest in, for instance, food packaging applications.

Keywords PHBV · PLA · PBAT · Reactive extrusion · Biopolymer blends

Introduction

The future scarcity of petroleum and the strong awareness of post-consumer plastic wastes are the two main drivers behind the interest, at both academic and industrial levels, in biopolymers. The terms "bio-based polymers" and "biodegradable polymers" are extensively used in the polymer literature when referring to biopolymers [1]. Bio-based polymers include both naturally occurring macromolecules, such as proteins and carbohydrates, and polymers synthetized from renewable monomers. Biodegradable polymers undergo rapidly and completely disintegration through the action of enzymes and/or chemical deterioration associated with living microorganisms. Articles fully made of biodegradable polymers can be also compostable according to the specifications of international standards (e.g. EN 13432 and ASTM D6400). Bio-based polymers can be either non-degradable, such as bio-based polyethylene (bio-PE) [2] and bio-based polyamides (bio-PAs) [3], or biodegradable polymers. Among biodegradable polymers, bio-based aliphatic polyesters, including polyhydroxyalkanoates (PHAs) and polylactides (PLAs), play a predominant role due to their potentially hydrolysable ester bonds. Some biodegradable polyesters can be produced from non-renewable petroleum resources, which is the case of, for instance, poly(butylene succinate) (PBS), poly(butylene succinate-*co*-adipate) (PBSA), and poly(butylene adipate-*co*-terephthalate) (PBAT) [4].

PHAs are aliphatic polyesters produced by bacterial fermentation with the highest potential to replace polyolefins. PHAs generally consist of 3–6 hydroxycarboxylic acids

✉ S. Torres-Giner
storreginer@iata.csic.es; storresginer@upv.es

1 Technological Institute of Materials (ITM), Universitat Politècnica de València (UPV), Plaza Ferrándiz y Carbonell 1, 03801 Alcoy, Spain

2 Novel Materials and Nanotechnology Group, Institute of Agrochemistry and Food Technology (IATA), Spanish Council for Scientific Research (CSIC), Calle Catedrático Agustín Escardino Benlloch 7, 46980 Paterna, Spain

and more than 150 monomers have been identified as their constituents [5]. Such diversity allows the production of biopolymers with a wide range of properties [6]. Poly(3-hydroxybutyrate) (PHB) homopolyester and its copolymer with 3-hydroxyvalerate (HV), i.e. poly(3-hydroxybutyrate-*co*-3-hydroxyvalerate) (PHBV) are the most important PHAs. The copolyester has lower crystallinity and stiffness while improved flexibility and toughness, broadening its processing window and applications [7]. However, most PHA materials cannot be easily processed in current processing equipment and are excessively rigid and brittle for a large number of packaging applications.

PLA also belongs to the family of aliphatic polyesters and it is synthetically produced in continuous via ring-opening polymerization (ROP) of the lactide dimer [8]. This monomer is habitually obtained from carbohydrate resources, including agricultural by-products [9]. Since it contains two chiral carbon centers, PLA can coexist in three stereochemical forms: poly(L-lactide) (PLLA), poly(D-lactide) (PDLA), and poly(DL-lactide) (PDLLA) [10]. Most commercial grades of PLA are indeed PLLA and PDLLA [11], which can be easily melt processed in conventional processing equipment, including film and sheet extrusion, injection molding, thermoforming, foaming, and fiber spinning, to frequently produce rigid articles [12]. However, the major drawbacks of PLA are related to its low heat distortion temperature (HDT) and toughness due to its low glass transition temperature (T_g ~ 60 °C) and intrinsic brittleness, respectively. To overcome these drawbacks, a large research activity is being carried out by melt mixing PLA with both natural fillers [13] and novel plasticizers [14].

PBAT is a semi-aromatic copolyester that is synthetically obtained by polycondensation reaction between 1,4-butanediol (BD) and a mixture of adipic acid (AA) and terephthalic acid (TPA), mainly derived from petroleum sources. A range from approximately 35–55 mol% TPA usually offers an optimal compromise between biodegradability and useful properties [15]. Because of their high flexibility, PBAT copolyesters are mostly interesting for flexible applications (e.g. bags and mulch films) [16]. In view of their high ductility, good heat resistance, and high-impact performance, blends of PBAT with other biopolymers, such as PLA [17], thermoplastic starch (TPS) [18], and PBS [19], have been studied.

Biodegradable polymers are suitable candidates for disposable material applications, particularly in short-term uses, such as packaging and hygiene. However, the use of biopolymers is currently restricted for most industrial applications due to both their poor processability as well as lower thermal stability and mechanical performance (when taken alone) than commodity polymers. Interestingly, the development of copolymers and biopolymer blends with satisfactory properties can straightforwardly overcome these limitations. In comparison to copolymerization, polymer blends represent an economic and more convenient way to provide the desired properties by physical mixing without any synthesis stage or chemical modification. However, most of the existing polymer blends are not thermodynamically miscible, which is mainly influenced by interactions such as dipole–dipole, ion–dipole, hydrogen bonding, acid–base, and donor and acceptor [20, 21]. As a result, immiscible polymer blends frequently need to be compatibilized in order to improve the adhesion between the phase components, reduce their interfacial tension, and generate limited inclusion phase sizes [22].

Compatibilization in biopolymer blends can be effectively addressed by either ex situ (non-reactive) or in situ (reactive) methods [22]. Ex situ compatibilization is based on the use of a premade (block or grafted) copolymer, being highly miscible with the blend components. However, this is a two-step strategy that is not habitually desirable from an industrial point of view and it is only suitable for specialty polymers where the cost of manufacturing and addition of the copolymer is economically feasible [23, 24]. In addition, it habitually yields a low compatibilizing effect due to it is almost impossible to reach all the added copolymer at the interface of the immiscible blend [25–27]. Alternatively, in situ compatibilization is performed by means of polymers, oligomers, and additives containing multi-functional groups (e.g. anhydride, epoxy, oxazoline, isocyanates, etc.). These are capable of reacting during melt processing with the hydroxyl and carboxyl functional groups of condensation polymers [28]. For this, it is important that the reactive compatibilizers have low melt viscosity so that they can easily diffuse to the blends interface within a short processing time [22].

In situ compatibilization of biopolymer blends with additives of low-molecular weight (M_W), such as reactive oligomers and oils, is both economically and environmentally favorable because it involves the use of a relatively low concentration of compatibilizer, typically below 5 wt%, in a one-step process [22, 29]. Recent studies have concluded that it results in the formation of in situ copolymers that improve drop breakup and stabilize coalescence in the blend systems [30, 31]. Among the studied reactive compatibilizers, epoxy-based styrene–acrylic oligomers (ESAOs) with different degree of functionalities and a relatively low M_W, well below 9000 g/mol, can easily form new ester bonds through reaction of their epoxy groups with the terminal functional groups of the biopolymer chains during melt processing. This mainly consists on glycidyl esterification of carboxylic acid end groups, which precedes hydroxyl end group etherification [32]. In ESAOs, styrene and acrylate building blocks are each typically 1–20 and 2–20, respectively, having glycidyl and epoxy groups incorporated as side chains [33]. By the epoxy ring-opening and subsequent

reaction with both the hydroxyl and carboxylic acid end groups, ESAOs can efficiently reconnect the biopolyester chains that break down during melt processing. These additives are indeed termed as "chain extenders" since the biopolyester chains are enlarged and the resultant M_W of the biopolymers is increased (or recovered if hydrolysis simultaneously occurs) [34]. The ESAOs-processed biopolymer articles typically present enhanced mechanical performance and thermal stability due to their increased M_W [35, 36]. Since the melt-processing time is frequently sufficient to accomplish chain reaction, this method is a straightforward methodology for achieving in situ compatibilization in polymer blends at industrial scale [37].

In ESAOs, the average number of epoxy groups per chain habitually lies between 4 and 9. This reactive oligomer can form in situ block copolymers by the hydrogen abstraction from the carboxyl group of blended polyesters [38]. However, most tested ESAO grades present high number average functionality (*f*), typically ~9, i.e. the so-called multifunctional ESAO (Joncryl® ADR 4368-C) [33], which can easily lead to the formation of highly chain-branched and/or cross-linked structures [38]. This may result in a dramatic reduction of the melt flow index (MFI) of the blended system, which could both limit its processing (e.g. injection molding) and originate gel formation (e.g. film extrusion). On the contrary, both bi-functional ESAO, i.e. with *f* values of ~2, and low-functionality ESAO, i.e. with *f* values of 4–5, can raise melt viscosity through linear chain-extension or moderate branching [39].

The present study reports, for the first time, the use of low-functionality ESAO to in situ compatibilize ternary blends of three commercial biodegradable polyesters, namely PHBV, PLA, and PBAT, by reactive extrusion (REX). These biopolymers were selected as they are currently produced in relatively large volumes and present a very dissimilar performance so that their combination can provide tunable properties for a broad range of packaging applications.

Experimental

Materials

Bacterial aliphatic copolyester PHBV was ENMAT™ Y1000P, produced by Tianan Biologic Materials (Ningbo, China). This biopolymer resin presents a density of 1.23 g/cm^3 and a melt flow index (MFI) of 5–10 g/10 min (190 °C, 2.16 kg). The HV fraction in the copolyester is 2–3 mol%.

Homopolyester PLA, grade Ingeo™ biopolymer 2003D, was obtained from NatureWorks (Minnetonka, MN, USA). Density is 1.24 g/cm^3 and MFI is ~6 g/10 min (210 °C, 2.16 kg). The D-lactide isomer content is 3.8–4.2 wt%.

Petrochemical copolyester PBAT, termed as Biocosafe 2003F, was purchased from Xinfu Pharmaceutical Co. Ltd. (Zhejiang, China). This resin presents a MFI value of ≤5 g/10 min (150 °C, 2.16 kg) and a density of 1.18–1.28 g/cm^3. The butylene adipate (BA)-to-butylene terephthalate (BT) ratio in the copolyester is approximately 55/45 (mol/mol).

Low-functionality ESAO was obtained from BASF S.A. (Barcelona, Spain), in the form of solid granules, under the trade name Joncryl® ADR 4300. Its M_W is 5500 g/mol, T_g is 56 °C, the epoxy equivalent weight (EEW) is 445 g/mol, and *f* is ≤5. Manufacturer recommends a dosage of 0.4–2 wt% for processing polyesters.

Melt Processing

Prior to processing, all biopolymer pellets were dried in an Industrial Marsé MDEO dehumidifier (Barcelona, Spain) at 60 °C for at least 12 h. Drying was necessary to minimize hydrolytic degradation of the biopolyesters.

The neat biopolymers and their ternary blends were melt-compounded in a co-rotating ZSK-18 MEGAlab laboratory twin-screw extruder from Coperion (Stuttgart, Germany). The screws feature 18 mm diameter with a length (L) to diameter (D) ratio, i.e. L/D, of 48. The biopolymer pellets and ESAO granules were manually pre-homogenized in a zipper bag and then fed into the main hopper. The materials dosage was set to achieve a residence time of about 1 min, measured by a blue masterbatch. The extrusion temperature profile, from the hopper to the die, was set as follow: 155, 160, 160, 165, 165, 170, and 175 °C. The strand was cooled in a water bath at 15 °C and pelletized using an air-knife unit.

Films with a mean thickness of 200–250 μm were obtained by thermo-compression in a hydraulic press 3850-model from Carver, Inc. (Wabash, IN, USA). The process was performed at 180 °C and 8 bar for 10 min, followed by fast cooling inside the press using an internal water system at 15 °C for 5 min. The films were stored at room conditions, i.e. 23 °C and 50% HR, for at least 15 days before characterization.

Table 1 summarizes the composition of the here-prepared biopolymer films. Addition of low-functionality ESAO was set at a fixed content of 2 parts per hundred resin (phr) of biopolymer.

Films Characterization

Morphology

The film cross-sections were observed by field emission scanning electron microscopy (FESEM) in a ZEISS ULTRA 55 from Oxford Instruments (Abingdon, United Kingdom).

Table 1 Films composition according to the weight content (wt%) of poly(3-hydroxybutyrate-*co*-3-hydroxyvalerate) (PHBV), polylactide (PLA), and poly(butylene adipate-*co*-terephthalate) (PBAT). Low-functionality epoxy-based styrene–acrylic oligomer (ESAO) was added as parts per hundred resin (phr) of biopolymer

Sample	PHBV (wt%)	PLA (wt%)	PBAT (wt%)	ESAO (phr)
PHBV	100	0	0	0
PLA	0	100	0	0
PBAT	0	0	100	0
PHBV/PLA/PBAT 1:1:1	33.33	33.33	33.33	0
PHBV/PLA/PBAT 1:1:1 + ESAO	33.33	33.33	33.33	2
PHBV/PLA/PBAT 2:1:1 + ESAO	50	25	25	2
PHBV/PLA/PBAT 3:1:1 + ESAO	60	20	20	2

Film specimens were cryo-fractured by immersion in liquid nitrogen and then mounted on aluminum stubs perpendicularly to their surface. The working distance (WD) varied in the 6–7 mm range and an extra high tension (EHT) of 2 kV was applied to the electron beam. Due to their non-conducting nature, samples were subjected to a sputtering process with a gold–palladium alloy in a sputter coater EMITECH-SC7620 from Quorum Technologies, Ltd. (East Sussex, United Kingdom). The sizes of the inclusion phase were determined using Image J Launcher v 1.41 and the data presented were based on measurements from a minimum of 20 FESEM micrographs per sample.

Infrared Spectroscopy

Chemical analyses on the film surfaces were performed using attenuated total reflection-Fourier transform infrared (ATR-FTIR) spectroscopy. Spectra were recorded with a Vector 22 from Bruker S.A. (Madrid, Spain) coupling a PIKE MIRacle™ ATR accessory from PIKE Technologies (Madison, USA). Ten scans were averaged from 4000 to 400 cm^{-1} at a resolution of 4 cm^{-1}.

Thermal Analysis

Main thermal transitions of the biopolymer films were obtained by differential scanning calorimetry (DSC) in a Mettler-Toledo 821 calorimeter (Schwerzenbach, Switzerland). An average sample weight ranging from 5 to 7 mg was subjected to a heating program from 30 to 200 °C at a heating rate of 10 °C/min in nitrogen atmosphere (66 ml/min). Standard sealed aluminum crucibles of a volume capacity of 40 µl were used. DSC runs were performed in triplicate.

Thermal stability was determined by thermogravimetric analysis (TGA) in a Mettler-Toledo TGA/SDTA 851 thermobalance. Samples, with an average weight between 5 and 7 mg, were placed in standard alumina crucibles of 70 µl and subjected to a heating program from 30 to 700 °C at a heating rate of 20 °C/min in air atmosphere. TGA experiments were performed in triplicate.

Thermomechanical Tests

Dynamic mechanical thermal analysis (DMTA) was conducted in a DMA-1 model from Mettler-Toledo, working in tension mode, single cantilever. Film samples sizing $10 \times 5 \times 0.2$ mm^3 were subjected to a temperature sweep program from −40 to 130 °C at a heating rate of 2 °C/min, an offset strength of 1N, an offset deformation of 150%, and a control deformation of 6 µm. DMTA tests were run in triplicate.

Mechanical Tests

Tensile tests of the films were carried out by analyzing standard samples (type-2), as indicated in ISO 527-3, with a total length and width of 160 mm and 10 mm, respectively. The tests were performed in a universal testing machine ELIB 30 from S.A.E. Ibertest (Madrid, Spain), equipped with a 5-kN load cell, and using specific pneumatic clamps at a cross-head speed of 5 mm/min. At least six specimens per sample were tested.

Permeability Tests

The water vapor permeability (WVP) was determined according to the ASTM 2011 gravimetric method. For this, 5 ml of distilled water were poured into a Payne permeability cup ($\varnothing = 3.5$ cm) from Elcometer Sprl (Hermalle-sous-Argenteau, Belgium). The films were placed in the cups so that on one side they were exposed to 100% relative humidity (RH), avoiding direct film contact with water. The cups containing the films were then secured with silicon rings and stored in a desiccator at 25 °C and 0% RH. Identical cups with aluminum foils were used as control samples to estimate water loss through the sealing. The cups were weighed periodically using an analytical balance with ±0.0001 g

accuracy. Water vapor permeation rate (WVPR), also called water permeance when corrected for permeant partial pressure, was determined from the steady-state permeation slope obtained from the regression analysis of weight loss data per unit area versus time, in which the weight loss was calculated as the total cell loss minus the loss through the sealing. WVP was obtained, in triplicate, by correcting the permeance by the average film thicknesses.

Limonene permeability (LP) was also determined according to ASTM 2011 gravimetric method. Similarly, 5 ml of D-limonene, obtained from Sigma-Aldrich S.A. (Madrid, Spain) with 98% purity, was placed inside the Payne permeability cups and the cups containing the films were stored under controlled conditions, i.e. 25 °C and 40% RH. Limonene permeation rate (LPR) was obtained from the steady-state permeation slopes. The weight loss was calculated as the total cell loss minus the loss through the sealing plus the water sorption gained from the environment measured in samples with no permeant. LP was calculated taking into account the average sheet thickness in each case, measuring three replicates per sample.

Oxygen permeability (OP) was obtained from the oxygen transmission rate (OTR) measurements using an Oxygen Permeation Analyzer M8001 from Systech Illinois (Thame, UK). The samples were previously purged with nitrogen in the humidity equilibrated samples and then exposed to an oxygen flow of 10 ml/min. The exposure area during the test was 5 cm^2. Test were performed at 25 °C and 60% RH and recorded in duplicate.

Results and Discussion

Morphology

Figure 1 shows the FESEM images, taken at low (left) and high (right) magnification, of the biopolymer film cross-sections obtained by cryo-fracture. As it can be seen in Fig. 1a–c, all neat biopolymer films presented a relatively homogenous fracture surface with different degrees of roughness. In the case of PHBV and PLA, shown in Fig. 1a, b, respectively, one can observe that both biopolymer films followed a similar pattern of breakage, showing a smooth surface that is representative of brittle materials. The fracture surface of the PLA film also presented certain plastic deformation, evidenced by the presence of long filaments. On the contrary, as seen in Fig. 1c, the PBAT film showed a considerably rougher surface. In this micrograph it can be observed that several micro-cracks were formed during the fracture.

In relation to the biopolymer blends, gathered in Fig. 1d–g, these exhibited heterogeneous surfaces that were based on an "island-and-sea" morphology in which a part

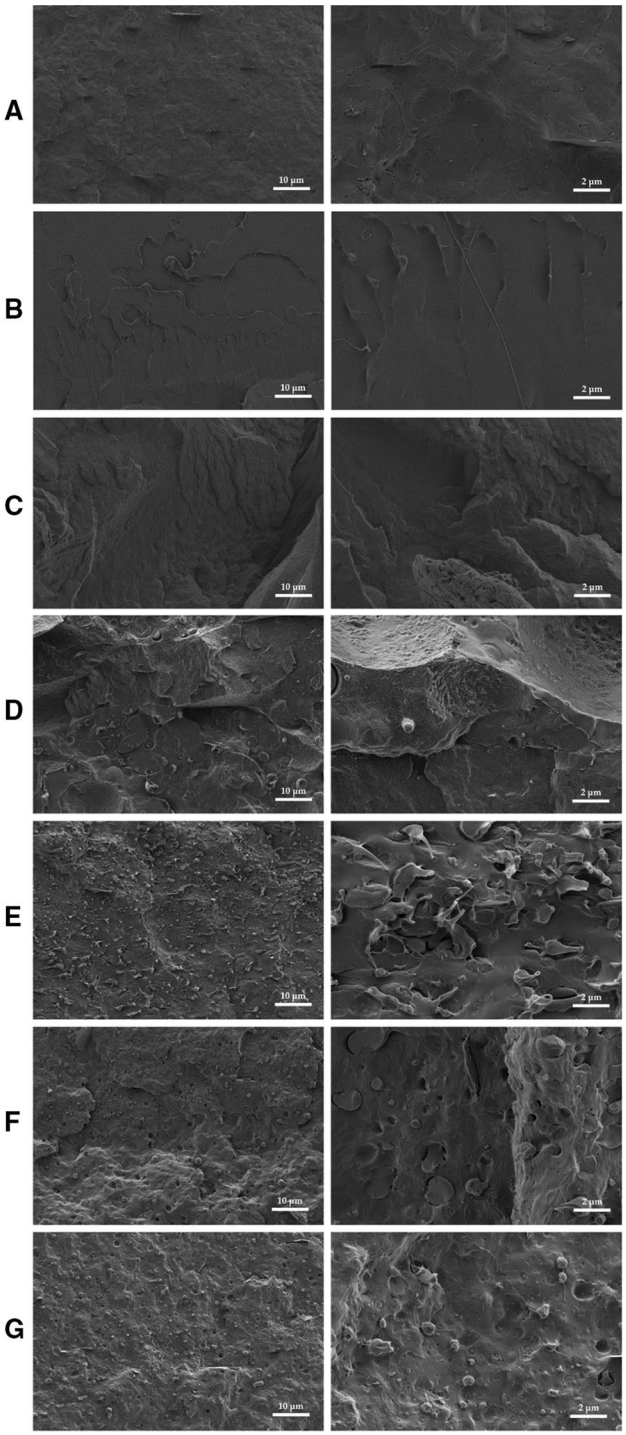

Fig. 1 Field emission scanning electron microscopy (FESEM) images of the cryo-fracture surfaces taken at 1000× (left) and 5000× (right) corresponding to the films made of: **a** Poly(3-hydroxybutyrate-*co*-3-hydroxyvalerate) (PHBV); **b** Polylactide (PLA); **c** Poly(butylene adipate-*co*-terephthalate) (PBAT); **d** PHBV/PLA/PBAT 1:1:1; **e** PHBV/PLA/PBAT 1:1:1 with low-functionality epoxy-based styrene–acrylic oligomer (ESAO); **f** PHBV/PLA/PBAT 2:1:1 with ESAO; **g** PHBV/PLA/PBAT 3:1:1 with ESAO

of each phase was dispersed as small droplets in the others. The absence of a co-continues phase morphology in the blends supports previous studies indicating that, at the here-studied mixing ratios, these biopolymers are thermodynamically immiscible [40]. However, the droplet sizes of the embedded inclusion phases were considerably larger in the ternary blend film processed without ESAO, in the range of 2–10 µm, as it can be seen in Fig. 1d. This indicates a rapid coalescence as well as a poor interface adhesion between the biopolymer phases. In the case of the ternary blend films melt processed with low-functionality ESAO, the inclusion phases were stretched into submicron droplets, i.e. lower than 1 µm, indicating that a higher coalescence stabilization of the biopolymer phases was achieved. As seen in Fig. 1g, for the ternary blend film melt processed with ESAO and with the highest PHBV content, i.e. 60 wt%, the droplets size achieved the lowest value, presenting a mean diameter of approximately 600 nm. This morphological change can be attributed to the achievement of a partial miscibility in the biopolymer ternary blends that, as one can expect, increased at the highest PHBV contents. A similar effect of ESAO was observed, for instance, by Ojijo et al. [38] on PLA/PBSA blends, in which the inclusion phase size was significantly reduced from 2.69 to 0.7 µm due to a reduced surface tension between the phases. A previous study consisting of PLA and PBAT blends compatibilized by ESAO also suggested that partial miscibility is achieved through the in situ formation of a block copolymer [41].

One can additionally observe that, after melt processing the ternary blends with ESAO, the fracture surface behavior of their films predominantly changed from brittle to ductile. In the case of the uncompatibilized blend film, i.e. the ternary blend melt processed without ESAO, it presented a clear pull-out of the inclusion phase after fracture, which is supported by the presence of large holes in Fig. 1d. However, the submicron droplets in the ternary blend films processed with ESAO induced a notable plastic deformation with, interestingly, no evidence of phase separation. Therefore, the addition of low-functionality ESAO also improved the adhesion between the blended components, expecting to facilitate a better stress transfer from one phase to another phase. In this sense, Lin et al. [42] also reported a significant adhesion improvement in PLA/PBAT blends by means of tetrabutyl titanate (TBT), which decreased the interface between the two biopolymers. Indeed, the resulting biopolymer binary blends only acquired improved performance when the stress transfer between the two blended components was effective. In another work, Arruda et al. [43] studied the morphology in both machine direction (MD) and transverse direction (TD) of a blown film made of PLA/PBAT processed with and without multi-functional ESAO. The incorporation of ESAO into the blend changed the PBAT inclusion phase shape, in both MD and TD, from a platelet-like to a refined fibrilar structure. This morphological change was specifically attributed to the improved compatibility between the phases due to the formation of a PLA-*b*-PBAT copolymer at the interface of both biopolymers.

Chemical Properties

FTIR was carried out in order to ascertain the chemical interactions of the biopolymer phases after the addition of low-functionality ESAO. Figure 2 shows the FTIR spectra of the low-functionality ESAO granules and the films of the ternary blend PHBV/PLA/PBAT 1:1:1 melt-processed with and without low-functionality ESAO. In the ESAO spectrum, the main peaks related to C–O stretching vibration of the epoxy groups appeared at ~ 1180, 910, and 840 cm^{-1} [33, 44–46]. These peaks were not observed in the spectrum of the ternary blend processed with low-functionality ESAO, indicating that the functional groups of the oligomer reacted and were consumed during melt compounding. In this sense, the ESAO reaction in a binary PLA/PBSA blend was previously confirmed by FTIR spectroscopy as a result of the disappearance of the epoxy group bands at 907 and 843 cm^{-1} [38].

In relation to the spectra of the biopolymers blend one can observe that the strongest band of the polyesters, attributed to their C=O stretching [13], slightly broadened and shifted from 1721 cm^{-1}, for the uncompatibilized ternary blend, to 1718 cm^{-1}, for the ternary blend melt processed with low-functionality ESAO. The shoulder of the carbonyl peak centered at ~ 1750 cm^{-1} also became more intense in the compatibilized sample. A similar peak change was

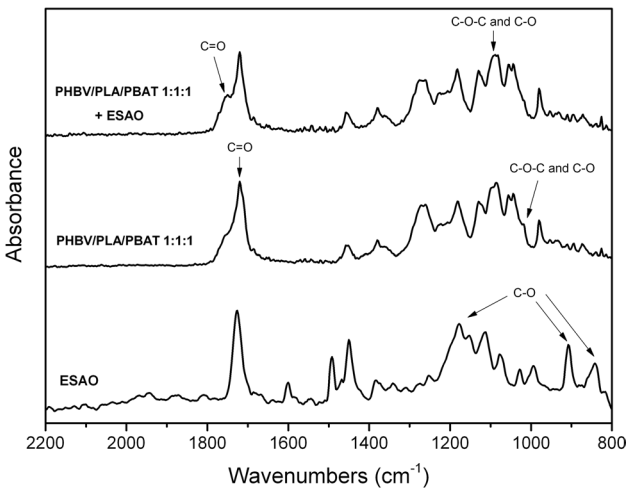

Fig. 2 Fourier transform infrared (FTIR) spectra, from bottom to top, of: low-functionality epoxy-based styrene–acrylic oligomer (ESAO) and the ternary blends of poly(3-hydroxybutyrate-*co*-3-hydroxyvalerate) (PHBV), polylactide (PLA), and poly(butylene adipate-*co*-terephthalate) (PBAT) processed without and with low-functionality ESAO. Arrows indicate the chemical bonds described in the text

previously ascribed to the reaction between the epoxy groups of multi-functional ESAO and the carboxyl groups (–COO) in polyesters [47]. This observation has been also related to a disruption of the hydrogen bonding in the molecular arrangement of the PHA chains [33], which further supports the presence of a newly formed copolyester. It is also worthy to mention the slight increase observed for the ester-related band at ~ 1080 cm^{-1} that was accompanied to the reduction of the band at ~ 1020 cm^{-1}, which are known to arise from C–O and C–O–C stretching vibrations of ester groups in biopolyesters [48]. Although these changes were subtle, they may suggest a reduction of the former ester bonds in the biopolymers as well as the formation of new ones.

According to the above-described chemical interactions, Fig. 3 proposes the chemical reaction of the three biopolymers with the epoxy functional groups of low-functionality ESAO during melt processing. The proposed scheme suggests the formation of a new copolyester, which first involves the ring-opening of epoxy groups in ESAO and their subsequent reaction with the carboxyl groups of the terminal acids of the biopolymers to create new covalent C–O–C bonds. This chain-linking process is considered to be mainly linear based on the fact that, on the one hand, the reaction rate between epoxy groups with the carboxyl groups in polyesters is about 10–15 times more favorable than with the hydroxyl groups [41] and, on the other, the here-selected ESAO inherently presents a low functionality. As a result, a linear block terpolymer consisting of PHBV, PLA, and PBAT chains, i.e. a PHBV-*b*-PLA-*b*-PBAT terpolymer, and the related copolymers based on binary combinations of thereof are proposed to be formed.

Thermal Properties

Figure 4 shows the DSC heating thermograms of the biopolymer films. One can observe that the neat PHBV film presented a sharp melting peak at ~ 175 °C, showing no evidences of cold crystallization during heating. For both PLA and PBAT, the curves showed a slight and poorly defined endothermic peak centered at 151 °C and 124 °C, respectively. This observation suggests that the neat PLA

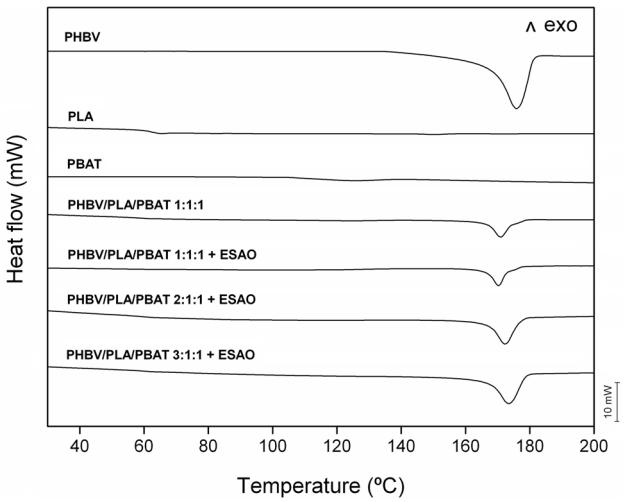

Fig. 4 Differential scanning calorimetry (DSC) thermograms of the ternary blend films made of poly(3-hydroxybutyrate-*co*-3-hydroxyvalerate) (PHBV), polylactide (PLA), and poly(butylene adipate-*co*-terephthalate) (PBAT) processed with and without low-functionality epoxy-based styrene–acrylic oligomer (ESAO)

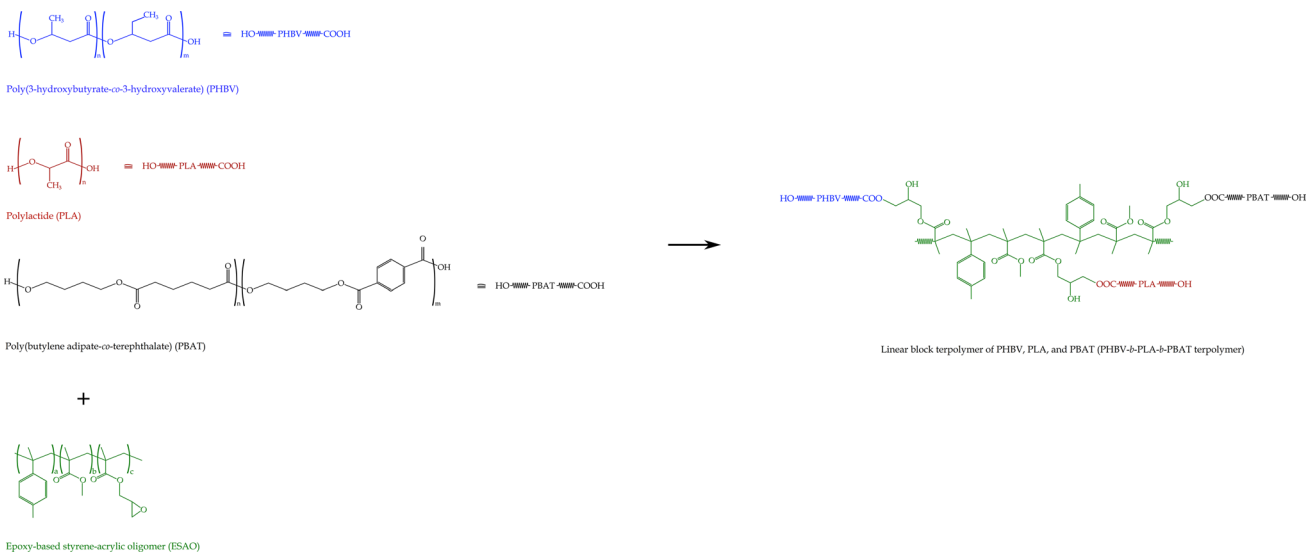

Fig. 3 Schematic representation of the in situ formed block terpolymer of poly(3-hydroxybutyrate-*co*-3-hydroxyvalerate) (PHBV), polylactide (PLA), and poly(butylene adipate-*co*-terephthalate) (PBAT) by low-functionality epoxy-based styrene–acrylic oligomer (ESAO). An average functionality (*f*) value of 3 was considered for the proposed reaction

and PBAT films were predominantly amorphous. Since the crystallization behavior is closely related to the biopolymers thermal history, it is considered that PLA and PBAT developed an amorphous structure at the cooling rate during the film production. In this sense, Miyata and Masuko [49] studied the non-isothermal crystallization of PLLA materials at various cooling rates, observing that samples cooled at rates greater than 10 °C min^{-1} did not crystallize and remained amorphous. In the case of the PLA film, T_g was observed at ~ 62 °C. This second thermal transition was not observed for the other biopolymer films as it is known to occur under ambient temperature, i.e. T_g ranges from − 40 to 5 °C for PHAs [6] while it is around − 20 °C for PBAT [19, 50]. In relation to the biopolymer ternary blend films, the DSC curves presented a low-intensity T_g in the 55–65 °C range and a melting process in the temperature range of 165–180 °C corresponding to their PLA and PHBV phases, respectively. Additionally, one can observe that low-functionality ESAO had no influence on the thermal transitions. However, it can be observed that the T_m values gradually increased with increasing the PHBV content, ranging from ~ 171 °C, for the 1:1:1 blend, to 174 °C, for the 3:1:1 blend. The melting enthalpies were also higher in the blend films with a higher PHBV content.

The results of the thermal stability of the biopolymer films are gathered in Fig. 5. Whereas Fig. 5a shows the TGA curves in the 100–700 °C range, their corresponding derivative thermogravimetric (DTG) curves are included in Fig. 5b. One can clearly observe that PHBV presented the lowest thermal stability, fully decomposing in a sharp single step. The values of onset degradation temperature, determined as the degradation temperature at 5% of mass loss ($T_{5\%}$), and degradation temperature (T_{deg}) were ~ 294 °C and 310 °C, respectively. On the contrary, both PLA and PBAT, particularly the latter, presented a relatively high thermal stability, showing $T_{5\%}$ values around 340 °C. Both biopolymers decomposed in two stages with T_{deg} values at approximately 390 °C and 480 °C, for PLA, and 430 °C and 510 °C, for PBAT. All ternary blend films showed a thermal stability profile relatively close to that of neat PHBV, though the onset was slightly delayed up to ~ 300 °C. It is also worthy to mention that the thermal decomposition of the blends occurred in three different stages in which the second mass loss, observed in the 325–375 °C range, can be mainly related to the PHBV phase. Therefore, the effect of the low-functionality ESAO addition on the thermal behavior and stability of the blends was relatively low, whereas the PHBV content played the major role in their thermal degradation.

Thermomechanical Properties

In order to fully determine the T_g of the biopolymer blends and also to further ascertain the potential effect of low-functionality ESAO on their miscibility, DMTA was carried out from − 40 to 130 °C. The evolution of the storage modulus, loss modulus, and damping factor (tan δ) as function of temperature of the biopolymer films are included in Fig. 6. The storage modulus is a measure of the energy stored and recovered in a cyclic deformation and it represents the stiffness of the films. As shown in Fig. 6a, at − 40 °C, the neat PHBV film showed a value of approximately 5600 MPa. This was significantly higher than those of PLA and PBAT, having values of 3450 MPa and 2400 MPa, respectively. The storage modulus of PHBV started to decrease at approximately 0 °C, which corresponds to the initiation of alpha (α)-transition region of this biopolymer. In the case of the PLA film, this thermomechanical change was observed at ~ 55 °C, while

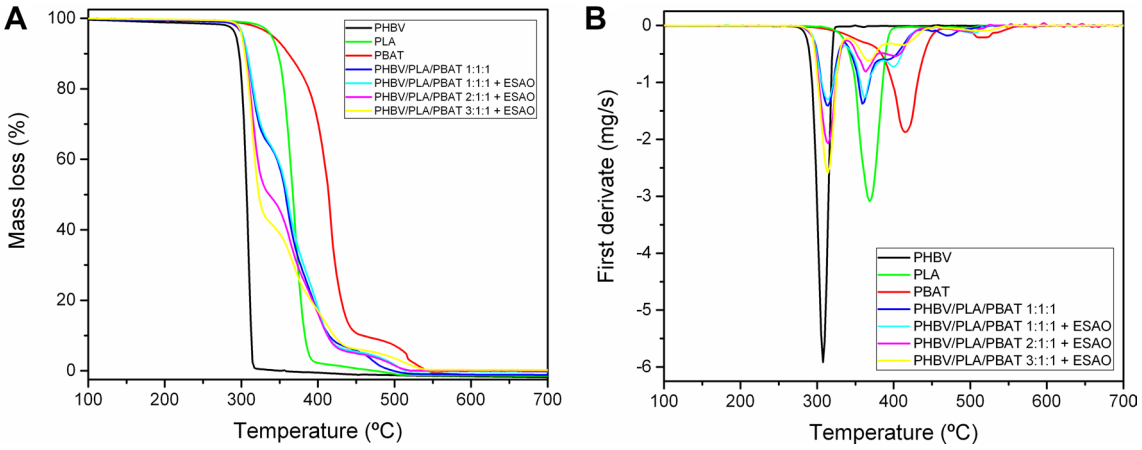

Fig. 5 **a** Thermogravimetric analysis (TGA) and **b** derivative thermogravimetric (DTG) curves of the ternary blend films made of poly(3-hydroxybutyrate-*co*-3-hydroxyvalerate) (PHBV), polylactide (PLA), and poly(butylene adipate-*co*-terephthalate) (PBAT) processed with and without low-functionality epoxy-based styrene–acrylic oligomer (ESAO)

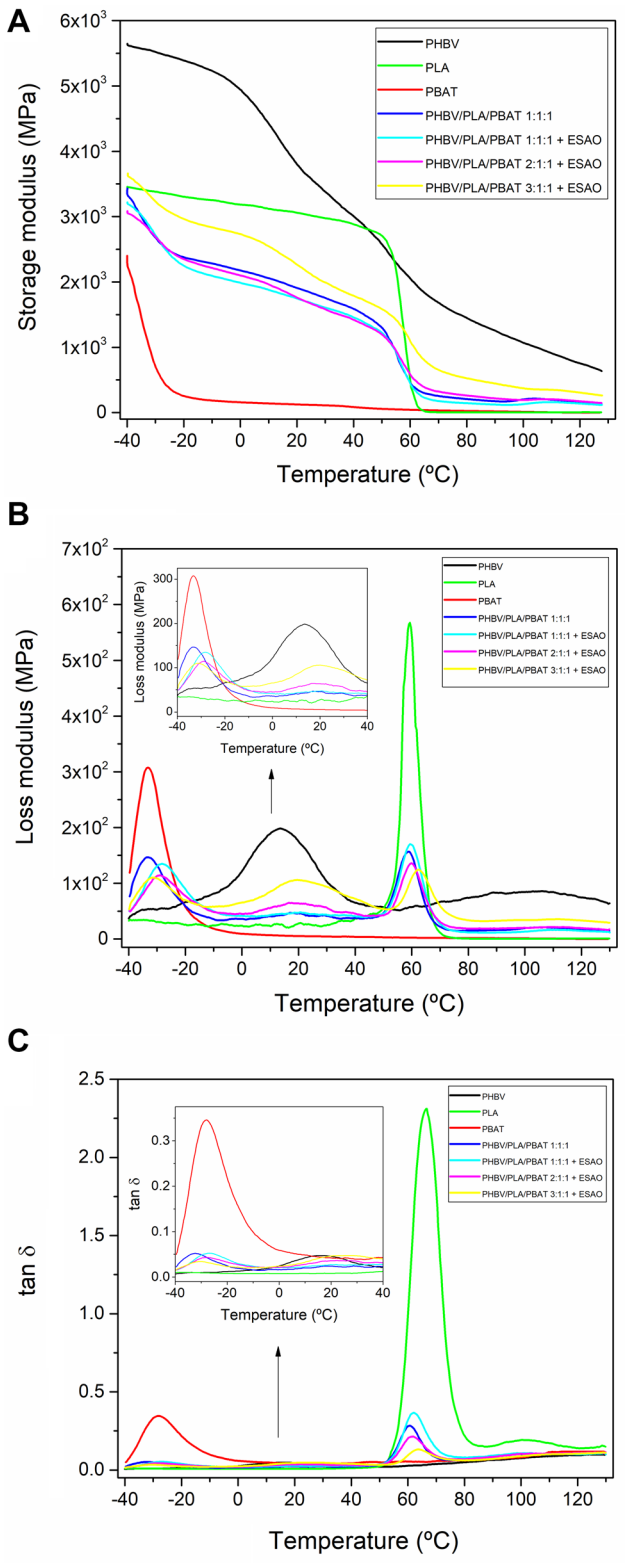

Fig. 6 Dynamic mechanical thermal analysis (DMTA) curves of the ternary blend films made of poly(3-hydroxybutyrate-*co*-3-hydroxyvalerate) (PHBV), polylactide (PLA), and poly(butylene adipate-*co*-terephthalate) (PBAT) processed with and without low-functionality epoxy-based styrene–acrylic oligomer (ESAO) in terms of: **a** Storage modulus; **b** Loss modulus; **c** Damping factor (tan δ)

for the PBAT film it overlapped with the beginning of the measurement, i.e. −40 °C. In addition, the reduction of the storage modulus at the α-transition region was more intense in the case of the PLA and PBAT films. This confirms that both more biopolymers were more amorphous, as previously described during DSC analysis, since a higher fraction of their molecules underwent the glass–rubber transition. Similar DMTA curves were reported for PLA and PBAT binary blends by Abdelwahab et al. [46], who also revealed that the addition of 1 phr ESAO increased the storage modulus for samples containing lignin. In the present study, all biopolymer blend films presented intermediate values of storage modulus, which increased as the PHBV content was increased. Comparison of the ternary blend with and without low-functionality ESAO indicated that the addition of the reactive oligomer slightly reduced the storage modulus, i.e. the film samples became more flexible. This effect was especially notable at low temperatures, indicating that low-functionality ESAO acted as a plasticizer.

The evolution of loss modulus versus temperature is depicted in Fig. 6b. These curves showed a sharp peak during the α-transition, which is related to the biopolymers T_gs and it is proportional to the energy increase that is dissipated in the films during the loading cycle. This further confirms that each biopolymer undergoes its glass–rubber transition at very different temperatures. The maximum values of loss modulus were particularly observed at approximately −34 °C (0.31 GPa), 13 °C (0.2 GPa), and 58 °C (0.56 GPa) for PBAT, PHBV, and PLA, respectively. In the case of the uncompatibilized blend, this film sample presented three α-peaks related to each biopolymer phase, at temperatures very similar to the ones observed for the neat biopolymers. Interestingly, the ternary blends compatibilized with low-functionality ESAO presented a clear shift of the α-peaks to intermediate temperatures compared to those of the neat biopolymers in the blend. For instance, the α-peak related to the PBAT phase of the 1:1:1 blend moved to −29.5 °C (0.13 GPa), i.e. an increase of 4.5 °C, after compatibilization. Similarly, the α-peak related to the PHBV phase increased to approximately 19 °C (0.05 GPa) in the compatibilized ternary blend films. Indeed, the study of T_g, in addition to morphology, can be efficiently used to differentiate the level of miscibility in polymer blends. Whereas thermodynamically immiscible blends show different distinguishable T_g values, blends made of two polymers that constitute a completely miscible blend present a single T_g and partially miscible blends have tendency to shift the T_g value of one component toward that of the other. The here-observed shifts of T_g after the addition of low-functionality ESAO thus support the partial miscibility of the ternary blends. In a similar way, Ren et al. [51] also observed a slight T_g decrease in binary and ternary blends of TPS, PLA, and PBAT with increasing contents of the latter biopolymer.

Analogous observations were found in Fig. 6c for the damping factor, which relates the ratio of the energy lost to the energy stored in a cyclic deformation. However, the peak displacements related to state changes in the films presented a lower intensity than in the case of the loss modulus. It is also worthy to note the enhancement observed in the tan δ peak with the addition of low-functionality ESAO. For instance, at 60 °C, it increased from a value of 0.275, for the uncompatibilized blend, up to a value of 0.36, in the case of the compatibilized blend by low-functionality ESAO, i.e. an improvement close to 30%. This directly implies a greater energy dissipation and improved toughness for the ternary blends processed with low-functionality ESAO [52].

Mechanical Properties of Ternary Blends

Figure 7 shows the tensile stress–strain curves at room temperature of the biopolymer films. The mechanical results, in terms of tensile modulus (E), tensile strength at yield (σ_y), and elongation at break (ε_b), are gathered in Table 2. One can observe that both PHBV and PLA biopolymers produced rigid films with relatively high values of E, i.e. 800–1200 MPa, and σ_y, i.e. 30–40 MPa. As a result, both biopolymers share some mechanical similarities with traditional rigid polymers, such as polyethylene terephthalate (PET), polystyrene (PS), polypropylene (PP), and polycarbonate (PC), making them very attractive to develop disposable and compostable rigid articles [53, 54]. However, these films were also very brittle, presenting values of ε_b lower than 6%, which limits their application in flexible packaging. In contrast, the PBAT film was very flexible and ductile, reaching ε_b values of ~900%. In this sense, it has been reported that PBAT has mechanical properties similar to that of low-density polyethylene (LDPE) [55].

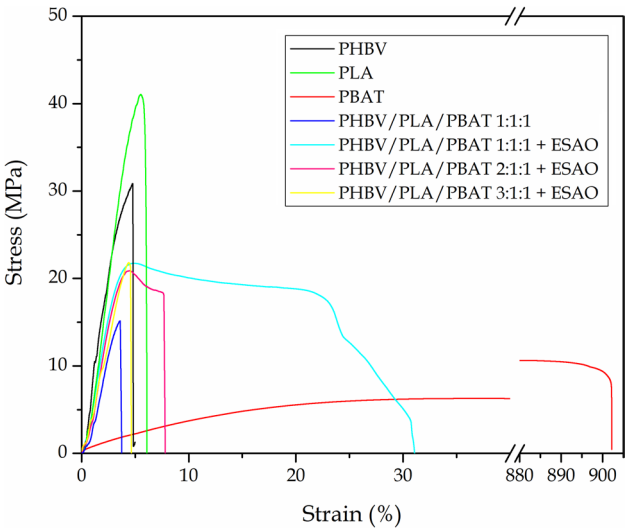

Fig. 7 Tensile stress–strain curves of the ternary blend films made of poly(3-hydroxybutyrate-*co*-3-hydroxyvalerate) (PHBV), polylactide (PLA), and poly(butylene adipate-*co*-terephthalate) (PBAT) processed with and without low-functionality epoxy-based styrene–acrylic oligomer (ESAO)

Table 2 Mechanical properties of the films made of poly(3-hydroxybutyrate-*co*-3-hydroxyvalerate) (PHBV), polylactide (PLA), and poly(butylene adipate-*co*-terephthalate) (PBAT) processed with and without low-functionality epoxy-based styrene–acrylic oligomer (ESAO) in terms of elastic modulus (E), tensile strength at yield (σ_y), and elongation at break (ε_b)

Sample	E (MPa)	σ_y (MPa)	ε_b (%)
PHBV	1151.2 ± 63.8	30.4 ± 1.2	2.1 ± 0.1
PLA	822.5 ± 18.3	39.6 ± 1.3	5.5 ± 0.3
PBAT	42.6 ± 1.5	11.6 ± 0.5	901.2 ± 39.6
PHBV/PLA/PBAT 1:1:1	583.1 ± 17.4	14.1 ± 0.9	4.4 ± 0.2
PHBV/PLA/PBAT 1:1:1 + ESAO	644.8 ± 29.6	19.1 ± 0.7	35.1 ± 1.6
PHBV/PLA/PBAT 2:1:1 + ESAO	756.8 ± 28.3	20.2 ± 0.8	7.2 ± 0.5
PHBV/PLA/PBAT 3:1:1 + ESAO	788.6 ± 23.7	21.0 ± 0.9	4.6 ± 0.3

Melt blending of the three biopolymers without low-functionality ESAO compatibilizer resulted in a film with intermediate mechanical strength values but still with poor ductility. Due to insufficient adhesion between the different phases, it is considered that the soft PBAT domains acted as stress concentrators since these present different elasticity, favoring mechanical failure during the tensile test. A similar effect was recently observed for uncompatibilized PLA/PBAT/PBS blends, in which the stress concentration resulted in a high triaxial stress in the PBAT domain that provoked debonding at the particle–matrix interface [56]. This observation correlates well with the FESEM images shown during the morphological analysis. Interestingly, the same ternary biopolymer blend melt processed with low-functionality ESAO presented higher mechanical values but also with an extraordinary improvement in ductility. In particular, after the addition of low-functionality ESAO to the PHBV/PLA/PBAT 1:1:1 blend, the E and σ_y values were improved by more than 10% and 35%, respectively, while ε_b value was almost 8 times higher. For the whole studied composition range, the use of higher contents of PHBV in the ternary blends gradually provided greater mechanical strength properties but also lower ductility. Therefore, the preparation of different mixing ratios resulted in biopolymer films with tunable mechanical properties.

The here-observed mechanical improvement is in agreement with some previous works related to biopolymer blends obtained by REX. For instance, the addition of either 2 or 5 wt% of glycidyl methacrylate (GMA) during melt compounding to an immiscible PLA/PBAT binary blend resulted in a toughness increase of the binary blend without severe

loss in tensile strength [57]. In another work, Ojijo et al. [38] also reported that the values of ε_b and impact strength of compression-molded PLA/PBSA 3:2 blend sheets improved from *ca*. 100 to 200% and from 9.8 to 34.7 kJ/m^2, respectively, with the incorporation of 1 phr multi-functional ESAO. More importantly, the blends also presented a relatively high tensile strength while simultaneously exhibiting improved thermal stability and favorable crystallinity. More recently, blown PLA/PBAT 8:2 films prepared by reactive blending with 1 phr multi-functional ESAO showed a ε_b value of ~ 250% [58]. Those binary blend films also possessed high E and σ_y values, i.e. 2 GPa and 50–60 MPa, respectively. However, in these previous studies the addition of multi-functional ESAO also resulted in a high increase of the melt viscosity, which could limit the industrial applicability of the biopolymer blends.

Barrier Properties of Ternary Blends

Table 3 shows the barrier properties in terms of WPV, LP, and OP for the here-developed biopolymer films. The barrier performance is, indeed, one of the main parameters of application interest in the food packaging field. Whereas both water vapor and oxygen barrier properties are important to avoid physical and chemical deterioration, limonene transport properties are usually used as a standard system to test aroma barrier. In the case of the neat biopolymers, one can observe that the PHBV film presented the highest barrier performance in relation to both water vapor and oxygen, showing WVP and OP values of approximately 1.8×10^{-15} kg m m^{-2} Pa^{-1} s^{-1} and 2.1×10^{-19} m^3 m m^{-2} Pa^{-1} s^{-1}, respectively. The PLA film showed the lowest LP value and intermediate values of WVP and OP, while the permeability values of the PBAT film were the highest. In this sense, it has been reported that the water vapor barrier of PLA is one order of magnitude lower than PS and PET [59]. Similarly, it has been reported that the oxygen barrier property of PBAT is around 50% lower than LDPE [55], which is already a low barrier material to oxygen. In the case of limonene, as opposed to moisture, this is a strong plasticizing component for PHAs and, then, solubility plays a key role in permeability. For instance, solvent-cast films of PHBV with 12 mol% HV have been reported to uptake up to 12.7 wt% limonene, reaching a LP value of ~ 2×10^{-13} kg m m^{-2} Pa^{-1} s^{-1} [60]. The here-obtained PHBV film was around 20× more barrier to limonene, which can be ascribed to both the preparation methodology and its lower HV content.

The biopolymer blend films presented intermediate barrier properties in comparison to the films made of the neat biopolymers. The PHBV/PLA/PBAT 1:1:1 blend film processed with low-functionality ESAO showed slightly higher WVP and LP values than the uncompatibilized blend film, but a significantly lower OP value. As supported above during the morphology analysis, low-functionality ESAO induced a reduction of the inclusion phase size and also of the interface of the biopolymer regions in the blend, which could favor plasticization by water and/or limonene vapors. Alternatively, since oxygen is a noncondensable small permeant, the presence of the newly formed PHBV-*b*-PLA-*b*-PBAT terpolymer may also reduce the free volume of the ternary blend and, then, delay the diffusion of the oxygen molecules. A previous work performed on the barrier properties of biopolymer blends has reported that PLA/poly(propylene carbonate) (PPC) cast films processed with 0.5 phr multi-functional ESAO exhibited optimal performance and certain compatibility, but it did not experience any positive influence on the WVP and OP compared to their corresponding uncompatibilized binary blend [47]. In general, increasing the content of PHBV in the biopolymer blends increased the barrier performance to both water vapor and oxygen, whereas it decreased the limonene barrier properties. In particular, the PHBV/PLA/PBAT 3:1:1 blend compatibilized by low-functionality ESAO showed the most balanced barrier performance. This biopolymer blend film presented WVP and OP values relatively similar to those of compression-molded films of petroleum-derived PET, i.e. 2.30×10^{-15} kg m m^{-2} Pa^{-1} s^{-1} and 1.35×10^{-19} m^{3}m m^{-2}

Table 3 Barrier properties of the films made of poly(3-hydroxybutyrate-*co*-3-hydroxyvalerate) (PHBV), polylactide (PLA), and poly(butylene adipate-*co*-terephthalate) (PBAT) processed with and without low-functionality epoxy-based styrene–acrylic oligomer (ESAO) in terms of water vapor permeability (WVP), LP, and OP

Sample	WVP×10^{15} (kg m m^{-2} Pa^{-1} s^{-1})	LP×10^{15} (kg m m^{-2} Pa^{-1} s^{-1})	OP×10^{18} (m^3 m m^{-2} Pa^{-1} s^{-1})
PHBV	1.82 ± 0.37	10.26 ± 0.57	0.21 ± 0.03
PLA	12.31 ± 0.98	3.30 ± 0.41	2.22 ± 0.24
PBAT	33.13 ± 1.46	72.58 ± 3.07	9.14 ± 0.86
PHBV/PLA/PBAT 1:1:1	5.11 ± 0.67	3.14 ± 0.82	1.31 ± 0.14
PHBV/PLA/PBAT 1:1:1 + ESAO	5.86 ± 0.29	3.73 ± 0.79	0.49 ± 0.03
PHBV/PLA/PBAT 2:1:1 + ESAO	4.78 ± 0.79	4.34 ± 0.37	0.35 ± 0.19
PHBV/PLA/PBAT 3:1:1 + ESAO	2.75 ± 0.68	4.99 ± 0.96	0.30 ± 0.18

$Pa^{-1}\ s^{-1}$, respectively, but a considerably lower LP value, i.e. 1.17×10^{-13} kg m m^{-2} Pa^{-1} s^{-1} [61, 62]. Therefore, a potential application of the here-developed biopolymer ternary blends in medium and medium-to-high barrier packaging applications are foreseen.

Conclusions

The present study describes the preparation and characterization of novel biopolymer ternary blends made of PHBV, PLA, and PBAT. The neat PHBV film, which was the major component of the blends, presented poor thermal stability, extremely low ductility, and low barrier to limonene (aroma) but high crystallinity, sufficient mechanical strength, and good barrier properties to water and oxygen. The incorporation of PLA improved both processability and aroma barrier while PBAT offered higher ductility and slightly better thermal stability. The resultant uncompatibilized biopolymer blends offered an intermediate mechanical and barrier performance, however these were immiscible and still presented a relatively low thermal stability and poor ductility.

The addition of low-functionality ESAO successfully increased the miscibility of the blended biopolymers, acting as a reactive compatibilizer during melt compounding. After the achievement of partial compatibilization, the coarse morphology of the soften inclusion phase in the immiscible blend changed to a finer morphology, inducing a more ductile fracture behavior. Although the effect of low-functionality ESAO on the thermal stability of the biopolymer blends was relatively low, this reactive additive provided enhanced overall mechanical performance, particularly in terms of ductility, as well as higher oxygen barrier. This enhancement was proposed to be achieved by the in situ formation of a newly linear PHBV-*b*-PLA-*b*-PBAT terpolymer and the copolymers of thereof, which were produced at the biopolymers interface due to reaction between the multiple epoxy groups of ESAO with the functional terminal groups of the biopolymers. Due to the inherently low functionality of ESAO and the more favorable reactivity of the epoxy groups with the carboxyl groups in polyesters, it is proposed that the reaction mainly produced a linear connection of the biopolymer chains, avoiding the formation of highly branched and/or cross-linked structures and facilitating the processability of the films.

Finally, the here-prepared biopolymer ternary blends presented different physical properties, depending on the selected mixing ratio. The ternary blends with the highest contents of PHBV share some similarities with traditional rigid polymers such as PET, PS, and PC, which makes them attractive as a sustainable alternative in the food packaging field for disposable and compostable articles. The resultant biopolymer articles can find potential uses as packaging materials requiring moderate barrier performance such as, among others, trays and containers to package fresh food.

Acknowledgements This research was funded by the EU H2020 project YPACK (Reference number 773872) and by the Spanish Ministry of Science, Innovation, and Universities (MICIU) with project numbers MAT2017-84909-C2-2-R and AGL2015-63855-C2-1-R. L. Quiles-Carrillo wants to thank the Spanish Ministry of Education, Culture, and Sports (MECD) for financial support through his FPU Grant Number FPU15/03812. Torres-Giner also acknowledges the MICIU for his Juan de la Cierva contract (IJCI-2016-29675).

References

1. Babu RP, O'Connor K, Seeram R (2013) Prog Biomater 2:8
2. Torres-Giner S, Torres A, Ferrándiz M, Fombuena V, Balart R (2017) J Food Saf 37:e12348
3. Quiles-Carrillo L, Montanes N, Boronat T, Balart R, Torres-Giner S (2017) Polym Test 61:421
4. Zakharova E, Alla A, Martínez A, De Ilarduya S, Muñoz-Guerra (2015) RSC Adv 5:46395
5. Steinbüchel A, Valentin HE (1995) FEMS Microbiol Lett 128:219
6. McChalicher CWJ, Srienc F (2007) J Biotechnol 132:296
7. Reis KC, Pereira J, Smith AC, Carvalho CWP, Wellner N, Yakimets I (2008) J Food Eng 89:361
8. Vink ETH, Davies S (2015) Ind Biotechnol 11:167
9. John RP, Nampoothiri KM, Pandey A (2006) Process Biochem 41:759
10. Madhavan Nampoothiri K, Nair NR, John RP (2010) Biores Technol 101:8493
11. Garlotta D (2001) J Polym Environ 9:63
12. Lim LT, Auras R, Rubino M (2008) Prog Polym Sci 33:820
13. Quiles-Carrillo L, Montanes N, Sammon C, Balart R, Torres-Giner S (2018) Ind Crops Prod 111:878
14. Quiles-Carrillo L, Blanes-Martínez MM, Montanes N, Fenollar O, Torres-Giner S, Balart R (2018) Eur Polym J 98:402
15. Witt U, Müller R-J, Deckwer W-D (1997) J Environ Polym Degrad 5:81
16. Siegenthaler KO, Künkel A, Skupin G, Yamamoto M (2012) Ecoflex® and Ecovio®: biodegradable, performance-enabling plastics. In: Rieger B, Künkel A, Coates GW, Reichardt R, Dinjus E, Zevaco TA (eds) Synthetic biodegradable polymers. Springer, Berlin Heidelberg, p 91
17. Jiang L, Wolcott MP, Zhang J (2006) Biomacromol 7:199
18. Brandelero RPH, Yamashita F, Grossmann MVE (2010) Carbohyd Polym 82:1102
19. Muthuraj R, Misra M, Mohanty AK (2014) J Polym Environ 22:336
20. Porter RS, Wang L-H (1992) Polymer 33(10): 2019
21. Koning C, Van Duin M, Pagnoulle C, Jerome R (1998) Prog Polym Sci 23:707
22. Muthuraj R, Misra M, Mohanty AK (2017) J Appl Polym Sci 135:45726
23. Ryan AJ (2002) Nat Mater 1:8
24. Wu D, Zhang Y, Yuan L, Zhang M, Zhou W (2010) J Polym Sci Part B 48:756
25. Kim CH, Cho KY, Choi EJ, Park JK (2000) J Appl Polym Sci 77:226
26. Supthanyakul R, Kaabbuathong N, Chirachanchai S (2016) Polymer 105:1
27. Na Y-H, He Y, Shuai X, Kikkawa Y, Doi Y, Inoue Y (2002) Biomacromolecules 3:1179
28. Zeng J-B, Li K-A, Du A-K (2015) RSC Adv 5:32546

29. Xanthos M, Dagli SS (1991) Polym Eng Sci 31:929
30. Sundararaj U, Macosko CW (1995) Macromolecules 28:2647
31. Milner ST, Xi H (1996) J Rheol 40:663
32. Villalobos M, Awojulu A, Greeley T, Turco G, Deeter G (2006) Energy 31:3227
33. Torres-Giner S, Montanes N, Boronat T, Quiles-Carrillo L, Balart R (2016) Eur Polym J 84:693
34. Lehermeier HJ, Dorgan JR (2001) Polym Eng Sci 41:2172
35. Liu B, Xu Q (2013) J Mater Sci Chem Eng 1:9
36. Eslami H, Kamal MR (2013) J Appl Polym Sci 129:2418
37. Loontjens T, Pauwels K, Derks F, Neilen M, Sham CK, Serné M (1997) J Appl Polym Sci 65:1813
38. Ojijo V, Ray SS (2015) Polymer 80:1
39. Frenz V, Scherzer D, Villalobos M, Awojulu AA, Edison M, Van Der Meer R (2008) Multifunctional polymers as chain extenders and compatibilizers for polycondensates and biopolymers. In: Technical papers, regional technical conference—society of plastics engineers, p. 3/1678
40. Utracki LA (2002) Can J Chem Eng 80:1008
41. Al-Itry R, Lamnawar K, Maazouz A (2012) Polym Degrad Stab 97:1898
42. Lin S, Guo W, Chen C, Ma J, Wang B (2012) Mater Des (1980–2015) 36: 604
43. Arruda LC, Magaton M, Bretas RES, Ueki MM (2015) Polym Test 43:27
44. Wang Y, Fu C, Luo Y, Ruan C, Zhang Y, Fu Y (2010) J Wuhan Univ Technol Mater Sci Ed 25:774
45. Wei D, Wang H, Xiao H, Zheng A, Yang Y (2015) Carbohyd Polym 123:275
46. Abdelwahab MA, Taylor S, Misra M, Mohanty AK (2015) Macromol Mater Eng 300:299
47. Sun Q, Mekonnen T, Misra M, Mohanty AK (2016) J Polym Environ 24:23
48. Torres-Giner S, Gimeno-Alcañiz JV, Ocio MJ, Lagaron JM (2011) J Appl Polym Sci 122:914
49. Miyata T, Masuko T (1998) Polymer 39:5515
50. Muthuraj R, Misra M, Mohanty AK (2015) J Appl Polym Sci 132:42189
51. Ren J, Fu H, Ren T, Yuan W (2009) Carbohyd Polym 77:576
52. Torres-Giner S, Montanes N, Fenollar O, García-Sanoguera D, Balart R (2016) Mater Des 108:648
53. Jamshidian M, Tehrany EA, Imran M, Jacquot M, Desobry S (2010) Compr Rev Food Sci Food Saf 9:552
54. Savenkova L, Gercberga Z, Nikolaeva V, Dzene A, Bibers I, Kalnin M (2000) Process Biochem 35:573
55. Costa ARM, Almeida TG, Silva SML, Carvalho LH, Canedo EL (2015) Polym Test 42:115
56. Zhang K, Mohanty AK, Misra M (2012) ACS Appl Mater Interfaces 4:3091
57. Zhang N, Wang Q, Ren J, Wang L (2009) J Mater Sci 44:250
58. Chinsirikul W, Rojsatean J, Hararak B, Kerddonfag N, Aontee A, Jaieau K, Kumsang P, Sripethdee C (2015) Packag Technol Sci 28:741
59. Auras R, Harte B, Selke S (2004) J Appl Polym Sci 92:1790
60. Sanchez-Garcia MD, Gimenez E, Lagaron JM (2008) Carbohyd Polym 71:235
61. Sanchez-Garcia MD, Gimenez E, Lagaron JM (2007) J Plast Film Sheeting 23:133
62. Lagaron JM (2011) Multifunctional and nanoreinforced polymers for food packaging. In: Multifunctional and nanoreinforced polymers for food packaging. Woodhead Publishing, Cambridge, p 1